Desalination and Water Treatment
www.deswater.com

doi: 10.1080/19443994.2015.1106345

57 (2016) 19727–19740
September

Taylor & Francis
Taylor & Francis Group

Chemical characteristics of chromophoric dissolved organic matter in stormwater runoff of a typical residential area, Beijing

Chen Zhao, Chong-Chen Wang*, Jun-Qi Li*, Chao-Yang Wang, Yan-Ru Zhu, Peng Wang, Nan Zhang

Key Laboratory of Urban Stormwater System and Water Environment (Ministry of Education), Beijing University of Civil Engineering and Architecture, Beijing 100044, China, Tel. +86 10 6832 2124; Fax: +86 10 6832 2128;
emails: zhaochen_90@foxmail.com (C. Zhao), chongchenwang@126.com (C.-C. Wang), lijunqi@bucea.edu.cn (J.-Q. Li), 15116946231@163.com (C.-Y. Wang), 644972597@qq.com (Y.-R. Zhu), wangpeng@bucea.edu.cn (P. Wang), 2538513150@qq.com (N. Zhang)

Received 9 February 2015; Accepted 30 September 2015

ABSTRACT

Stormwater runoff acts as a vital intermediate between wet precipitation, terrestrial, and aquatic ecosystems, in which chromophoric dissolved organic matter (CDOM) plays an important role in influencing the transport, toxicity, bioavailability, and ultimate fate of many pollutants. It is important and necessary to characterize the CDOM in stormwater runoff, which is useful to clarify the relationship between CDOM with the other coexisting organic and/or inorganic components. In this study, 30 stormwater runoff samples were collected from three different stormwater events in a typical residential area in Beijing, and CDOM in the samples was characterized by UV–visible spectroscopy, excitation–emission matrix fluorescence and proton nuclear magnetic resonance (^{1}H NMR) spectroscopy to investigate its compositions, structures, and sources. Being compared to the previous studies on wet precipitation, average molecular weight of CDOM in this study was much larger, implying the presence of more aromatic components with carbonyl, carboxyl, hydroxyl and unsaturated carbon atoms functional groups. Furthermore, both allochthonous and autochthonous sources contributed to the local CDOM, and their chemical properties were influenced by anthropogenic and biogenic factors. Thus, the CDOM in stormwater runoff is a compositionally different matrix than that discovered in wet precipitation.

Keywords: Stormwater runoff; CDOM; Chemical composition; Structure; Source

1. Introduction

Chromophoric dissolved organic matter (CDOM) is an active component of total dissolved organic matter (DOM), which is ubiquitous in aquatic systems and can absorb both visible and UV light [1–4]. It has been widely investigated in aquatic systems during last decades [3–5]. Previous studies have demonstrated that CDOM is the dominant chromophore in wet precipitation, being involved in a variety of photomediated processes in the atmosphere [2]. Additionally, some CDOM constituents are surface-active, leading to produce a significant impact on droplet population and consequently cloud albedo via lowering the surface tension of atmospheric waters [6–8]. Being compared to

*Corresponding authors.

the wet precipitation, stormwater runoff possesses more complicated pollutants because it can not only flush a large amount of suspended materials [9], but also dissolve a significant proportion of nutrients and organic compounds [10,11], like total nitrogen (TN), total phosphorus (TP) and CDOM [12–14]. CDOM can also strongly bind organic and inorganic pollutants, and further heavily influence the transport, transformation, bioavailability, toxicity, and ultimate fate of above-stated pollutants [15,16]. Therefore, CDOM play vital role in various biochemical and physical processes. Up to now, little is known regarding the chemical characteristics and sources of CDOM in stormwater runoff, although McElmurry et al. explored the different compositions of DOM exported as stormwater from suburban and urban sources to investigate the influence of land cover and environmental factors on the DOM [17]. It is important and necessary to investigate the chemical properties of CDOM in stormwater runoff, as it acts as intermediate between atmospheric water and terrestrial and aquatic ecosystems [18].

In this study, UV–visible spectroscopy was used to evaluate the CDOM compositions and structures [2,3,5,17,19,20]. Excitation–emission matrix (EEM) fluorescence spectroscopy was applied to distinguish the CDOM types and to gain insight into their chromophoric nature [1,5,19–22]. Finally, ^{1}H NMR spectroscopy was introduced to provide information regarding hydrogen distributions and major functional groups presented in CDOM and their relative abundances, confirming the relative aliphatic and aromatic characteristics of CDOM [19,20,23].

2. Materials and methods

2.1. Stormwater runoff sampling and sample preparation

Stormwater runoff samples were collected on 29 July, 28 August, and 2 September of 2014, respectively, at a fixed sampling station of Dongluoyuan residential area (39˚51′N, 116˚24′E), which is a typical residential area close to the southern third ring road of Beijing, capital of China. This residential area has a population of around 6,500, with an annual mean temperature of 11–14˚C (the coldest, January: −4.6˚C; the hottest, July: 25.8˚C on average) [24]. The annual mean rainfall is 585 mm (the rainy season, between June and September, concentrating 85% of the annual rainfall), and the annual mean evaporation is 467 mm for land surfaces [24]. The underlying surface material is asphalt concrete pavement. Stormwater event of 29 July, 28 August and 2 September were labeled as event *A*, event *B*, and event *C*, respectively. Meteorological data, including rain amounts, rain duration, surface temperature, relative humidity, pressure and watershed area, were also recorded as described in Table 1.

Glass bottles (600 mL) were used to collect stormwater runoff samples. At each stormwater event, 10 samples were collected at the time of 0, 3, 6, 9, 14, 19, 24, 34, 44, and 59 min, after the start of runoff (t = 0 min) [17]. Each sample was labeled by the sampling sequence of the corresponding stormwater event (*A*#, *B*#, and *C*#), where *A*, *B*, and *C* represented event *A*, event *B*, and event *C*, respectively, and # corresponded to the sample number.

Prior to use, all glass wares used were soaked in a solution of NaOH (0.1 M) for 30 min, then washed with distilled water, followed by another immersion in a solution of HNO_3 (4 M) for 24 h, and finally washed with ultra-pure water with a resistivity of 18 megaohm cm^{-1} (Milli-Q). After collection, all stormwater runoff samples were transported to the laboratory within a few hours (<6 h) and stored in glass bottles in the dark at 4˚C for a maximum of 4 d, which was proved to be adequate for keeping the optical properties of the samples unchanged [5,19,20,23].

2.2. Dissolved organic carbon

The concentrations of total carbon (TC) and total inorganic carbon (TIC) of each stormwater runoff sample were determined by a Jena multi N/C 3100 analyzer. The DOC contents of the samples were theoretically calculated as the difference TC − TIC. For TC quantification, standards were prepared from reagent grade potassium hydrogen phthalate plus reagents grade sodium hydrogen carbonate and sodium carbonate in ultrapure water in the range of 1–100 mg C L^{-1}. For TIC measurements, standards were performed from reagents grade sodium hydrogen carbonate plus sodium carbonate in ultrapure water in the range of 1–50 mg C L^{-1}. Control standards were generally within 5% agreement in terms of TC and TIC content. For each sample, three replicates were analyzed for determining the DOC content [19,20].

2.3. UV–visible spectroscopy

UV–visible spectra of stormwater runoff samples were recorded on a PerkinElmer lambda 650S spectrophotometer in the range of 200–600 nm. Due to the CDOM concentration of stormwater runoff in this study is much higher than in wet precipitation, 1 cm quartz cell rather than 10 cm quartz cell was selected to perform the UV–visible analysis [19,20]. Ultrapure water (Milli-Q) was used as a blank.

Table 1
The meteorological data of the three events

Events	Rain amounts (mm)	Rain duration (min)	Relative humidity (%)	Pressure (in Hg)	Watershed area (m^2)	Surface temperature (°C)
Event *A*	32.4	178.0	92.0	29.35	855	22
Event *B*	20.6	165.0	95.5	29.71	855	21
Event *C*	25.4	156.0	94.4	29.61	855	20

2.4. EEM fluorescence spectroscopy

Fluorescence characteristics of the stormwater runoff samples were investigated by a Hitachi F-7000 Fluorescence spectrophotometer equipped with a Xenon flash lamp, using 1 cm quartz cell. Fluorescence measurements were conducted by making emission scans from 200 to 550 nm, at excitation wavelengths from 200 to 550 nm every 5 nm, with operating parameters of a 10 nm slit width, a PMT voltage of 700 V and scanning speed at 1,200 nm min^{-1}. Quinine sulfate in 0.05 mol L^{-1} H_2SO_4 was introduced as the reference standard with its minimum detection limit of 0.4 ppb in this fluorescence spectrophotometer. The relative fluorescent intensities of the samples were expressed in terms of standard quinine sulfate units (QSU), where 55.5, 58.3, and 56.7 intensity unit are equivalent to one QSU (1 QSU = 1 μg L^{-1} = 1 ppb in 0.05 mol L^{-1} H_2SO_4) for event *A*, event *B*, and event *C*, respectively [25,26]. As fluorescence data are often plagued by scattering effects, mainly Rayleigh and Raman scatter, which can overlap some useful fluorescent information. In this study, Rayleigh scatter effects were removed from the data-set by adding zero to the EEMs in the two triangle regions ($E_m \leq E_x + 20$ nm and $\geq 2E_x - 10$ nm) [27], and Raman scatters were eliminated from all spectra by subtracting the ultrapure water blank spectra [19]. The resulting map represented the specific fingerprints for the stormwater runoff samples.

In order to assess the sources, the degree of maturation and influence by autochthonous biological activity of CDOM, three fluorescence indices, namely the fluorescence index (FI), the humification index (HIX), and the biological index (BIX) were calculated using the Eqs. (1)–(3):

$$\mathrm{FI} = f_{450}/f_{500} \quad (1)$$

$$\mathrm{HIX} = H/L \quad (2)$$

$$\mathrm{BIX} = f_{380}/f_{430} \quad (3)$$

where f_{450} and f_{500} are the fluorescence intensity at the emission wavelength 450 and 500 nm at the excitation wavelength 370 nm, respectively [28–30]. *H* and *L* are the integral values from 435 to 480 nm and 300 to 345 nm at the excitation wavelength 254 nm, respectively [1,31,32]. And f_{380} and f_{430} are the fluorescence intensity at the emission wavelength 380 and 430 nm at the excitation wavelength 310 nm, respectively [1,30,32].

2.5. ^1H NMR spectroscopy

Prior to the ^1H NMR spectroscopy analysis, CDOM was isolated and extracted from 100 mL runoff samples filtered through hydrophilic PVDF Millipore membrane filters (0.45 μm) with a flow rate of 2 mL min^{-1} using Agilent Vac Elut SPS 24 solid-phase extraction equipment with Bond Elut C-18 sorbent. Two 5 mL aliquots of ultrapure water were passed through the cartridges after the stormwater runoff sample to remove residual salts. The samples were then eluted off the C-18 cartridges with 6 mL aliquots of 10% water in methanol. Following elution, solvent was removed under reduced pressure for 30 min [23]. The samples were transferred to 15-mL glass vials and dried under nitrogen atmosphere by Termovap Sample Concentrator (YGC-1217, Bao Jing Company) [33]. For NMR analysis, the solid extracts of the samples were dissolved in D_2O (Jin Ouxiang Company).

The ^1H NMR spectra were recorded on an Agilent 500 M DD2 NMR spectrometer with an operating frequency of 499.898 MHz. The acquisition of spectra was performed with a contact time of 2.045 s and with the standard s2pul pulse sequence. The recycle delay was 1 s and the length of the proton 90° pulses was 10.8 μs. About 256 scans were collected for each spectrum. A 1.0 Hz line broadening weighting function and baseline correction was applied. The identification of functional groups in the NMR spectra was based on their chemical shift (δ_H) relative to that of the water (4.7 ppm) [20].

3. Results and discussion

3.1. UV–visible spectroscopy

UV–visible spectroscopy is an important tool to evaluate the composition and structure of CDOM [19,20]. The UV–visible spectra of the stormwater runoff samples collected from three stormwater events were shown in Fig. 1. For all samples, the decrease in absorbance with increasing wavelength follows a trend similar to that already observed for wet precipitation samples [5,19,34], aerosol samples [35], and other samples of natural humic substances [36]. Compared with the other two events, the spectra of CDOM in the event *C* exhibited some additional visible small shoulders in the region of 250–300 nm, which can be attributed to phenolic, aromatic carboxylic and polycyclic aromatic compounds ($\pi \rightarrow \pi^*$ transition) [37,38]. Generally, the composition of stormwater runoff is extremely random and fluctuant due to the influence of traffic conditions [39], atmospheric wet precipitation [25] and human factors [40], which was affirmed by the UV–visible absorbance of CDOM in the samples collected from three events in this study.

In order to investigate the nature of the CDOM chromophores and to get information about the molecular weight of CDOM, the spectral slope coefficients (S), a parameter inferred from the obtained UV–visible spectra, was used to show how efficiently CDOM absorbs light as a function of the wavelength. Generally, the S values possessed a strongly negative correlation with molecular weight of CDOM [19,20,41]. However, the S values varied with the wavelength range over which it was calculated. For example, Jamieson et al. calculated S values within the spectra 275–295 nm to characterize the biochar-derived CDOM isolated from soil [41], and Stedmon et al. calculated S values within the spectra 300–650 nm to explore the molecular weight of CDOM in Danish coastal waters [42]. The S values (μm^{-1}) were calculated from nonlinear least-square regressions of the absorption

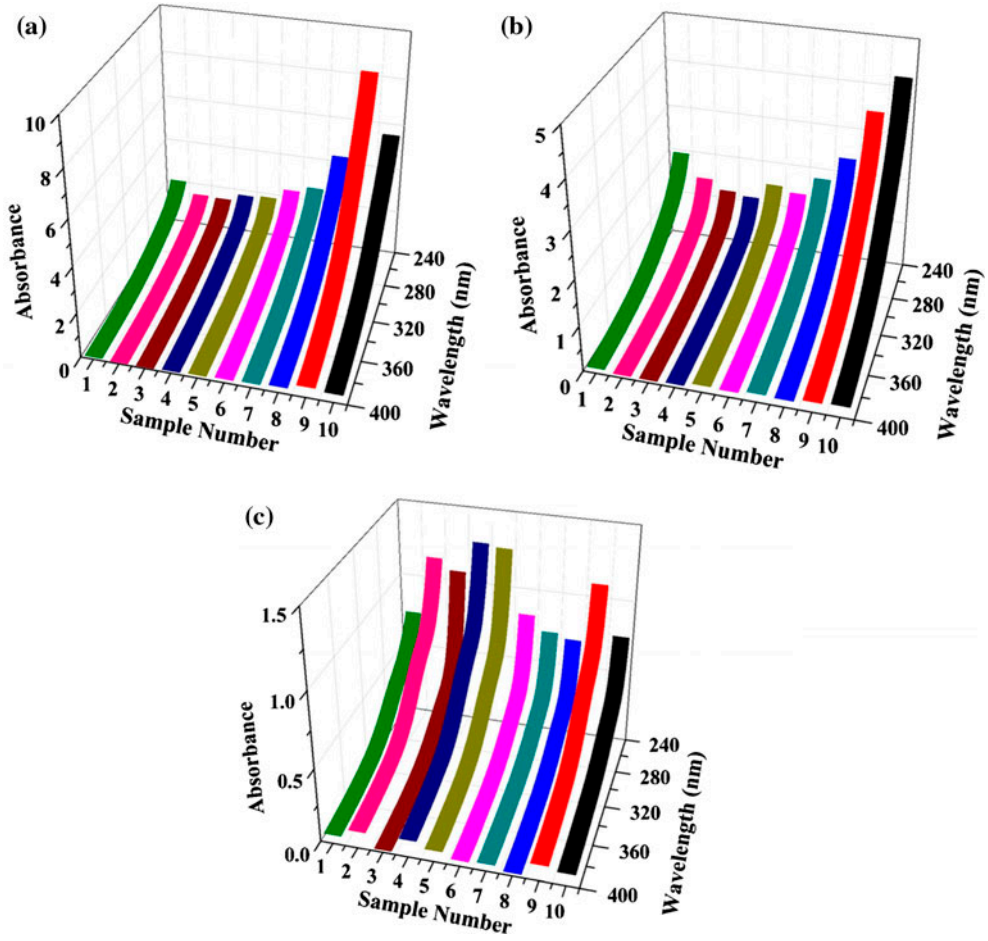

Fig. 1. UV–visible spectra of the three events samples: (a) event *A*, (b) event *B*, and (c) event *C*.

coefficients a_λ versus wavelength ranging from 240 to 400 nm following Eqs. (4) and (5):

$$a_\lambda = a_{\lambda_0} e^{S(\lambda_0-\lambda)} + K \quad (4)$$

$$a_\lambda = 2.303\, A_\lambda / l \quad (5)$$

where a_λ is absorption coefficients, A_λ is the absorbance reading at wavelength λ (nm), l (m) is the optical path length (0.01 m in this study), a_{λ_0} is the absorption coefficients at reference wavelength, λ_0 is the reference wavelength (300 nm was selected in this study), λ is the selected wavelength (ranging 240–400 nm), and K is a background parameter to improve the goodness of fitting. The median of S values determined for the CDOM in stormwater runoff samples of three events (event A, event B, and event C) were 17.34, 16.66, and 14.61 μm^{-1}, respectively. The S values in this study were much lower than those reported for wet precipitation [2,5,19,20], suggesting that the CDOM in the stormwater runoff samples collected from three events had higher molecular weight [5].

To further compare the molecular weight of the three events samples, M (the average molecular weight) were introduced as listed in Eq. (6):

$$M = a_{250}/a_{365} \quad (6)$$

where a_{250} and a_{365} are the absorption coefficients at 250 and 365 nm, respectively. As molecular size increases, the M value decreases because of stronger light absorption by high-molecular-weight CDOM at longer wavelengths [43]. As shown in Table 2, the median values of M were 7.72, 6.63, and 5.27 for event A, event B, and event C, respectively, suggesting the average molecular weight of CDOM followed the order of event C > event B > event A, which were also consistent with the S values, as listed in Table 2.

The aromaticity of CDOM in the three events was also evaluated via $SUVA_{280}$ (L mg C^{-1} m^{-1}), which can be calculated using the Eq. (7):

$$SUVA_{280} = a_{280}/DOC \quad (7)$$

where a_{280} is the absorbance coefficient measured at 280 nm (m^{-1}) [17]. In this study, the value of $SUVA_{280}$ was used to investigate the aromaticity rather than $SUVA_{254}$ [44], considering the facts of (i) for conjugated systems like those in aromatic molecules and other humic such as organic substances, the electrons can transfer from an overlapping π-orbital to the other one at 280 nm, (ii) some dissolved species (like nitrate, iron ions), which are ubiquitous in natural waters, achieved few absorption of UV light at 280 nm, and (iii) $SUVA_{280}$ was shown to linearly increase with aromatic carbon content in previous studies [17,44,45].

The median values of $SUVA_{280}$ (5.63, 7.06, and 14.35 L mg C^{-1} m^{-1} for event A, event B, and event C, respectively) were higher than those of DOM in stormwater runoff with different land covers reported by McElmurry et al. [17], implying that the CDOM in our study contained a greater amount of aromatic structure. The CDOM's $SUVA_{280}$ values of the three storm events were depicted in Fig. 2, which demonstrated more aromatic structures arose along with the stormwater runoff. Previous studies proposed that different landscapes were likely to produce different types of CDOM [17,46], therefore, being compared with more natural surface in suburban, farmland, and forest [47], our results could roughly demonstrate that asphalt concrete pavement was more prone to produce the aromatic substances. Furthermore, the vehicle exhaust [48], landfill leachate [49], atmospheric polycyclic aromatic hydrocarbons [50–52] washed by the wet precipitation and so on could also be the possible sources of aromatic substances of stormwater runoff. However, the values of $SUVA_{280}$ of event C were much higher than the other two events, suggesting there were more aromatic substances produced in event C. In order to obtain more detailed information about the types and structures of CDOM in the three events, further research should be carry out in the subsequent studies.

3.2. EEM fluorescence spectroscopy

Up to now, EEM fluorescence spectroscopy is a powerful technique to provide information about molecular size, chemical composition and aromacity or aliphatic properties of CDOM [22,27,53]. EEM fluorescence spectra of all three events samples were depicted in Figs. 3–5. Two major peaks could be identified from the three events fluorescence spectra. The first major peaks were located at E_x/E_m of 245–267 nm/389–398 nm, 242–265 nm/383–394 nm, and 261–267 nm/373–386 nm (peak A) in event A, event B, and event C, respectively, suggesting that UV humic-like substances were the major fluorophores components in the CDOM of runoff samples [53]. The second obvious peaks were observed at E_x/E_m of 224–227 nm/337–335 nm (peak T) only in event C, which could be attributed to tryptophan protein-like components [53]. The presence of tryptophan protein-like substances further confirmed that much more CDOM with larger molecular weight presented in

Table 2
The values of S and M of the three events

Sample	S (μm^{-1})	M	Sample	S (μm^{-1})	M	Sample	S (μm^{-1})	M
*A*1	18.15	9.39	*B*1	17.23	7.28	*C*1	15.25	6.09
*A*2	19.68	12.22	*B*2	17.77	7.69	*C*2	14.02	4.47
*A*3	19.24	10.44	*B*3	17.37	6.93	*C*3	17.83	10.20
*A*4	17.46	8.31	*B*4	15.56	5.47	*C*4	13.82	4.54
*A*5	15.65	5.92	*B*5	13.99	4.35	*C*5	14.98	5.71
*A*6	16.46	6.33	*B*6	14.28	4.55	*C*6	16.06	6.38
*A*7	15.43	6.34	*B*7	14.60	4.74	*C*7	14.24	4.82
*A*8	17.31	7.54	*B*8	16.32	6.33	*C*8	16.57	8.72
*A*9	17.36	7.90	*B*9	16.99	7.00	*C*9	13.61	4.58
*A*10	16.71	7.24	*B*10	17.44	7.46	*C*10	12.16	3.68

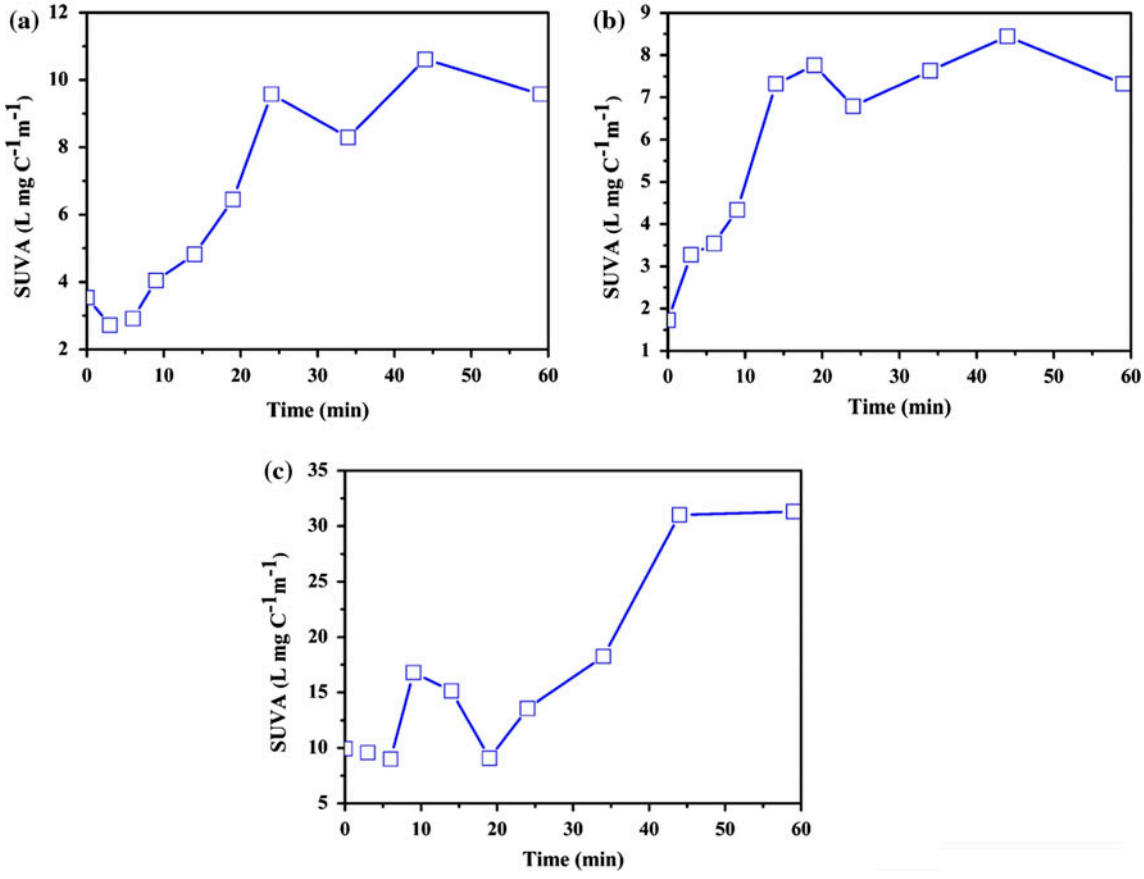

Fig. 2. Development of $SUVA_{280}$ values during storm event of three regions: (a) event *A*, (b) event *B*, and (c) event *C*.

event *C* [54,55]. Moreover, the fluorescence intensities of peak *A* in three events (event *A*, event *B*, and event *C*) varied from 483 to 3,533 QSU, 313 to 2,072 QSU and 140 to 368 QSU, respectively. The peak T fluorescence intensities of event *C* samples varied from 120 to 295 QSU. The values of QSU of samples in this study were much higher than those in previous studies about wet precipitation [1], because more chromophoric molecules were present in these stormwater runoff samples.

The FI, HIX and BIX values of the stormwater runoff samples in three events were listed in Table 3. The FI values of three events samples were 1.24–1.65, 1.32–1.78, and 1.44–1.89 for event *A*, event *B*, and

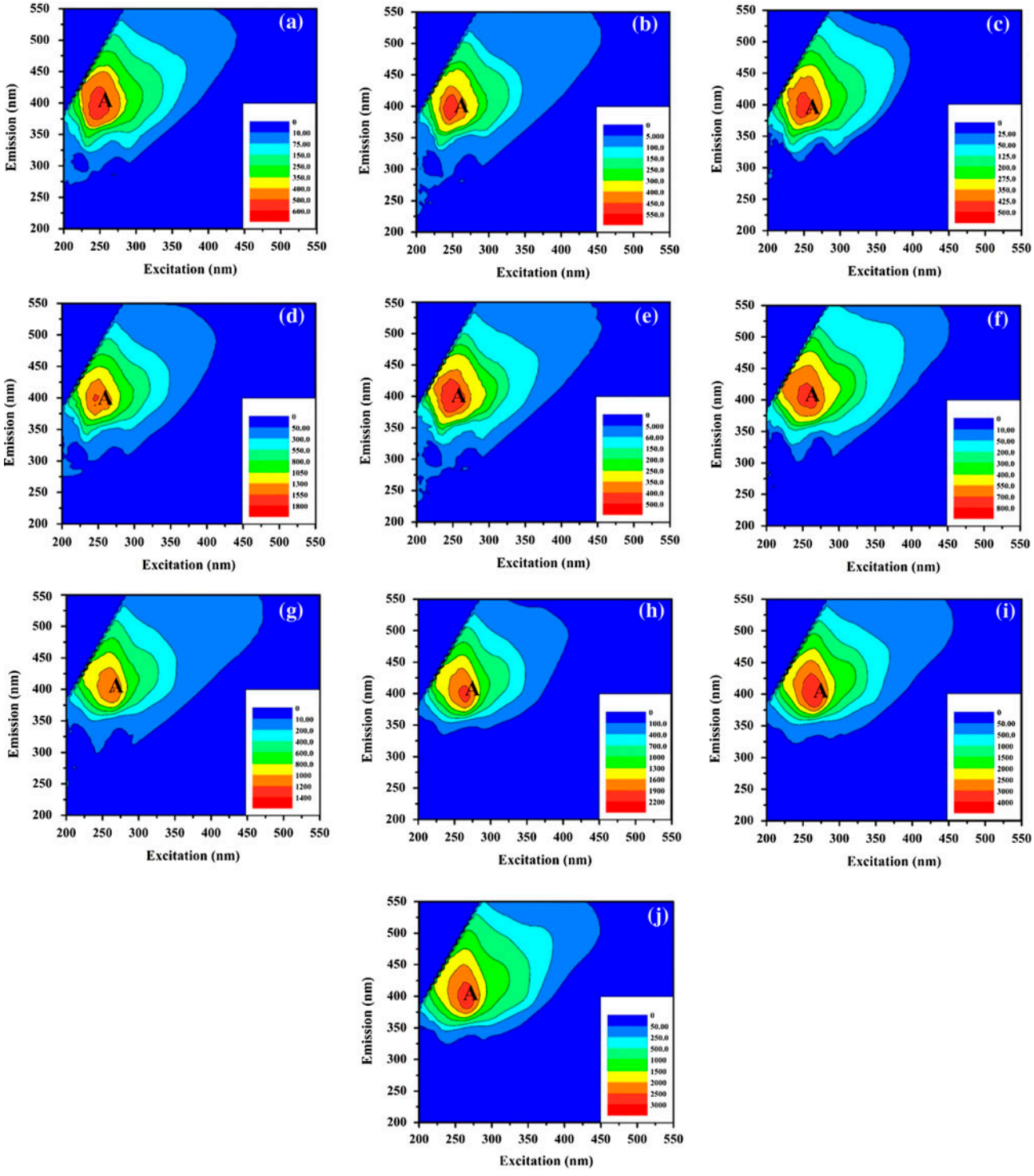

Fig. 3. EEM fluorescence contour profiles of the samples of event *A*: (a)–(j) corresponded to the sample numbers 1–10.

event *C*, respectively, suggesting that the sources of CDOM in the runoff samples were consistent with both terrestrial and microbial sources [28,29]. The values of HIX (10–16) had been the indicator of the strongly humic organic substances (terrestrial origin), whereas low values (<4) represented autochthonous organic components [1,30,32]. In our study, the HIX values were in the range of 3.49–22.86 and 2.33–10.50

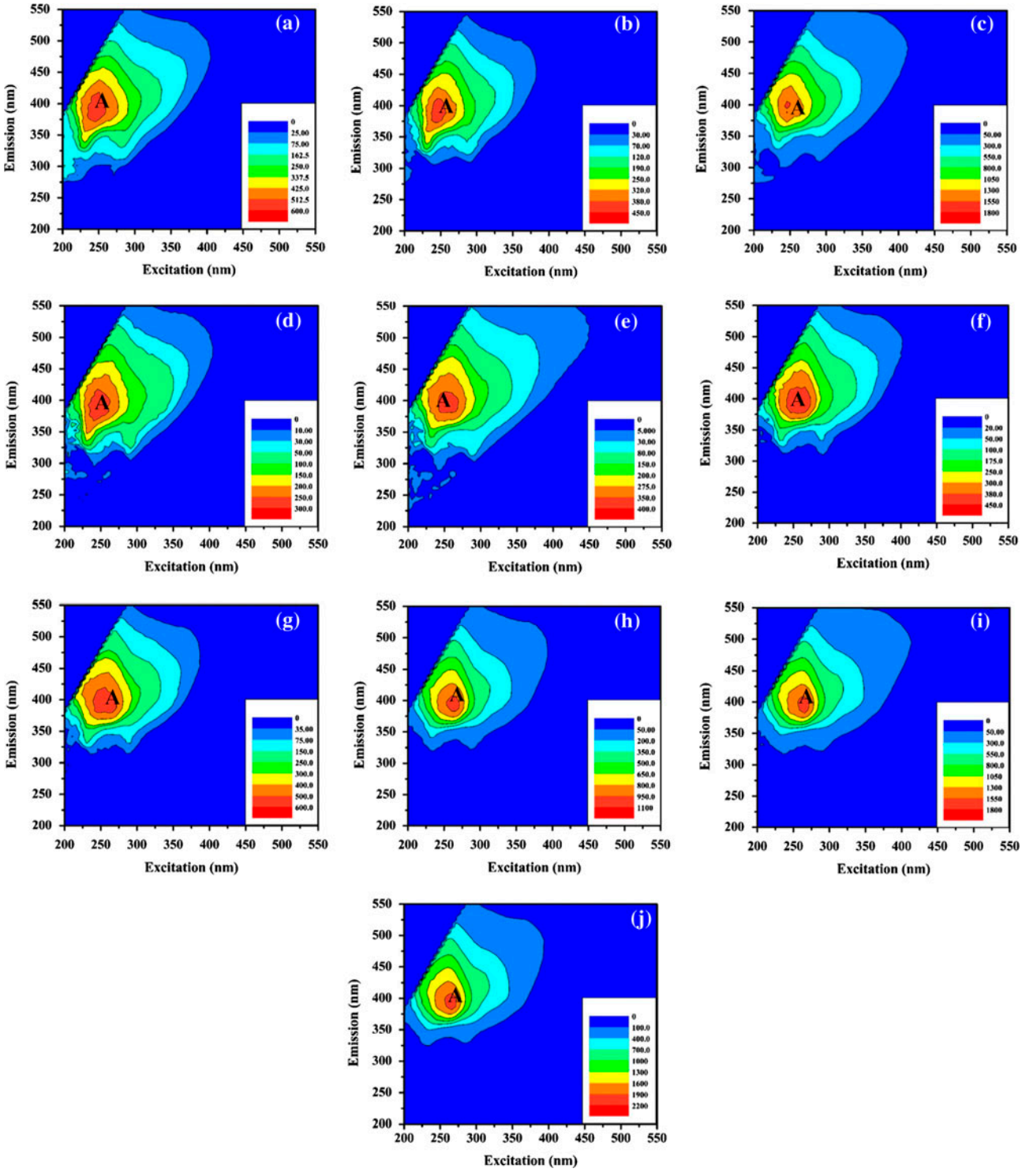

Fig. 4. EEM fluorescence contour profiles of the samples of event *B*: (a)–(j) corresponded to the sample numbers 1–10.

for event *A* and event *B*, respectively, implying that the CDOM in event *A* and B contained both allochthonous and autochthonous organic materials. While the CDOM in event *C* was assumed to be composed of autochthonous organic materials with lower HIX values ranging from 1.18 to 4.05.

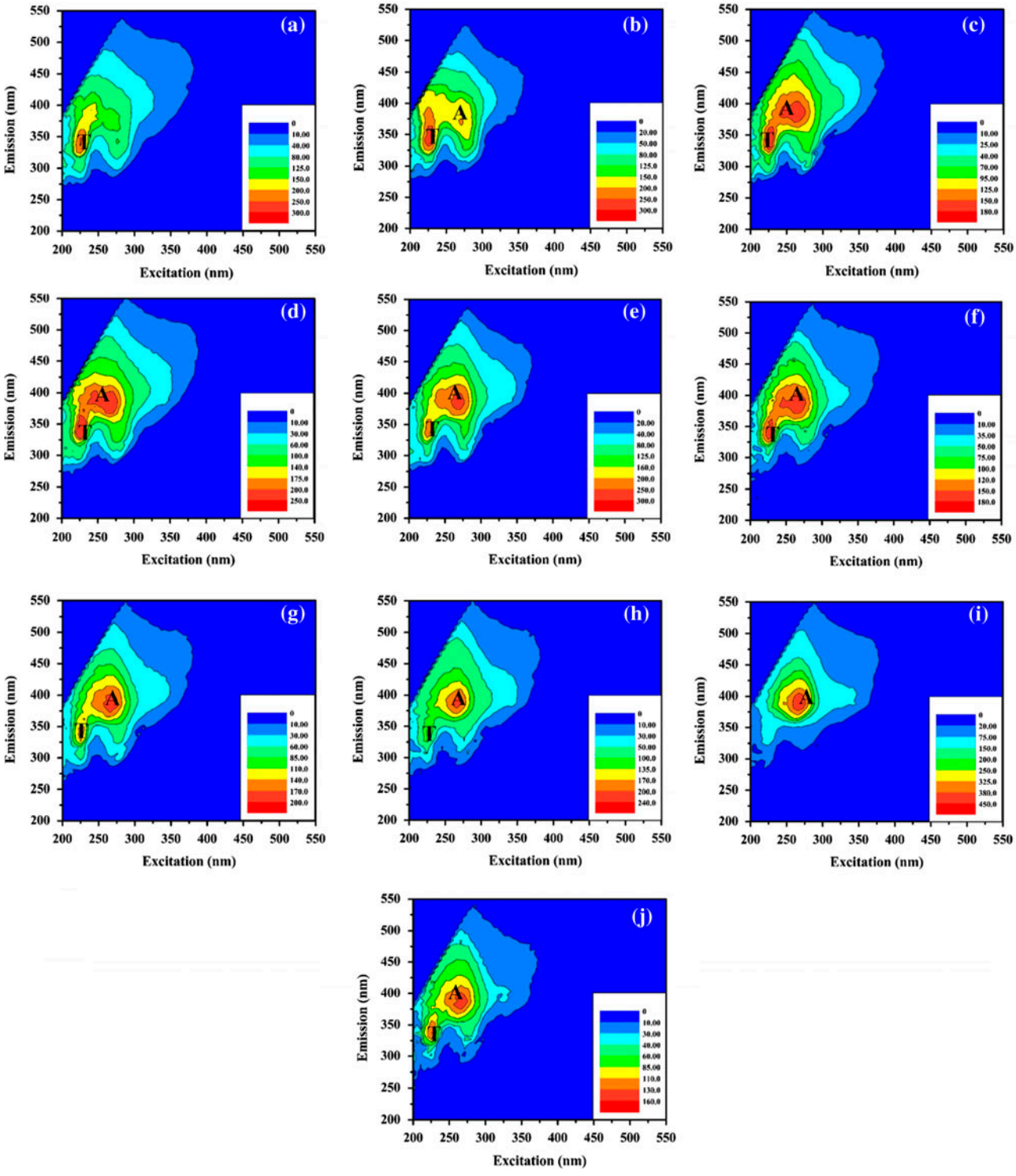

Fig. 5. EEM fluorescence contour profiles of the samples of event *C*: (a)–(j) corresponded to the sample numbers 1–10.

Previous study reported that the allochthonous organic matter sources are products of incomplete decomposition of plant and animal residues, while the autochthonous organic components may originate from the photosynthesis, which can be assessed by BIX values [1]. High BIX values (>1) corresponded to

Table 3
Fluorescence indices for runoff samples in the three events

Event	Sample	FI	HIX	BIX
Event *A*	*A*1	1.65	3.49	0.88
	*A*2	1.52	3.75	0.86
	*A*3	1.54	4.05	0.81
	*A*4	1.55	3.85	0.83
	*A*5	1.57	3.52	0.84
	*A*6	1.29	8.29	0.62
	*A*7	1.24	12.29	0.63
	*A*8	1.26	16.10	0.60
	*A*9	1.25	22.86	0.57
	*A*10	1.24	19.51	0.63
Event *B*	*B*1	1.75	2.63	0.96
	*B*2	1.63	2.54	0.99
	*B*3	1.78	2.33	1.02
	*B*4	1.61	2.48	0.98
	*B*5	1.44	3.65	0.85
	*B*6	1.35	4.29	0.87
	*B*7	1.46	4.40	0.80
	*B*8	1.32	7.30	0.78
	*B*9	1.39	10.12	0.74
	*B*10	1.36	10.50	0.73
Event *C*	*C*1	1.89	1.18	1.14
	*C*2	1.76	1.24	1.11
	*C*3	1.60	1.67	1.23
	*C*4	1.59	1.66	1.18
	*C*5	1.53	1.87	1.20
	*C*6	1.68	1.78	1.29
	*C*7	1.55	1.75	1.38
	C8	1.55	2.11	1.41
	*C*9	1.44	4.05	1.35
	*C*10	1.66	1.71	1.31

autochthonous sources, and low BIX values (<1) implied low abundance of organic matter of biological origin [1,30,32]. The BIX values of three events samples in this study were 0.57–0.88, 0.73–1.02, and 1.11–1.41 for event *A*, event *B*, and event *C*, respectively, suggesting the event *C* contained much more organic compounds from autochthonous and biological origin, which were consistent with its lower HIX values.

3.3. ^{1}H NMR spectroscopy

Proton NMR spectroscopy (^{1}H NMR) has become the most powerful analytical tools to characterize the water-soluble organic carbon (WSOC) composition of atmospheric aerosols [56–58] and the wet precipitation CDOM [2,5,19,20,23]. Much different from UV–visible and EEM fluorescence spectroscopy, ^{1}H NMR can provide the structural information via the corresponding integrated areas and the chemical shifts (δ_H) [19,20]. In this study, the samples of *A*1, *B*1, and *C*1 were selected as the representatives to carry out ^{1}H NMR analysis, and the results were demonstrated in Fig. 6(a). The spectra exhibited some distinct peaks overlaying much broader bands, implying the existence of complex mixtures of structures in the DOM. Although there were large varieties of overlapping resonances, each ^{1}H NMR spectrum was investigated on the basis of the chemical shift assignments described in the literature for aerosols and wet precipitation DOM [6,57]. Overall, integrated regions in the ^{1}H NMR spectra were: δ_H = 0.6–1.8 ppm (aliphatic protons, H–C); δ_H = 1.8–2.6, and 2.8–3.2 ppm (aliphatic protons in α position to carbonyl groups or unsaturated carbon atoms, H–C–C=); δ_H = 3.2–4.1 ppm (aliphatic protons on carbon atoms singly bound to oxygen atoms, H–C–O); and δ_H = 6.5–8.5 ppm (aromatic protons) [20].

The distribution of the different types of protons estimated from the partial integrals of the observed ^{1}H NMR regions for each sample was illustrated in Fig. 6(b). Being compared to the previous studies about wet precipitation, the results of the three samples exhibited similar patterns in terms of functional group composition, revealing predominance of aliphatic structures [5,18–20].

Firstly, the saturated aliphatic structures were found to be the major moieties (31–48%) in the three samples. Signals assigned to CH_3-terminal methyls (0.5–1.1 ppm) and CH_2 in alkyl chains (1.1–1.9 ppm) were also found in all the spectra. Apparently, the content of saturated aliphatic substances was slightly higher in sample *B*1 (48%) than the other two samples (40 and 31% for sample *A*1 and *C*1, respectively), which were consistent with the previous studies on wet precipitation [19,20].

Secondly, in the regions of δ_H = 1.8–2.6 and 2.8–3.2 ppm, the most prominent signals in the spectra of Fig. 6(a) arose from aliphatic protons linked to carbon atoms adjacent to C=C (including aromatic rings) or C=O double bonds [19,20], which accounts for 24–27% of the total integrated area of the spectra. However, as the sample *B*1 contained lower content of aromatic structures as illustrated in Fig. 6(b), along with the absence of the signal assigned to the vinylic protons in the δ_H = 5.0–6.5 ppm region, it was suggested that the compounds with the hydrogen atoms in α position to carbonyls and carboxyls groups were the dominant compositions. On the contrary, being compared with sample *B*1, the sample *A*1 and *C*1 had more hydrogen atoms in aromatic rings. And δ_H = 3.2–4.1 ppm region accounted for 16–21% of the total integral of the spectra, indicating the presence of the functional groups of hydroxyl groups of polyols

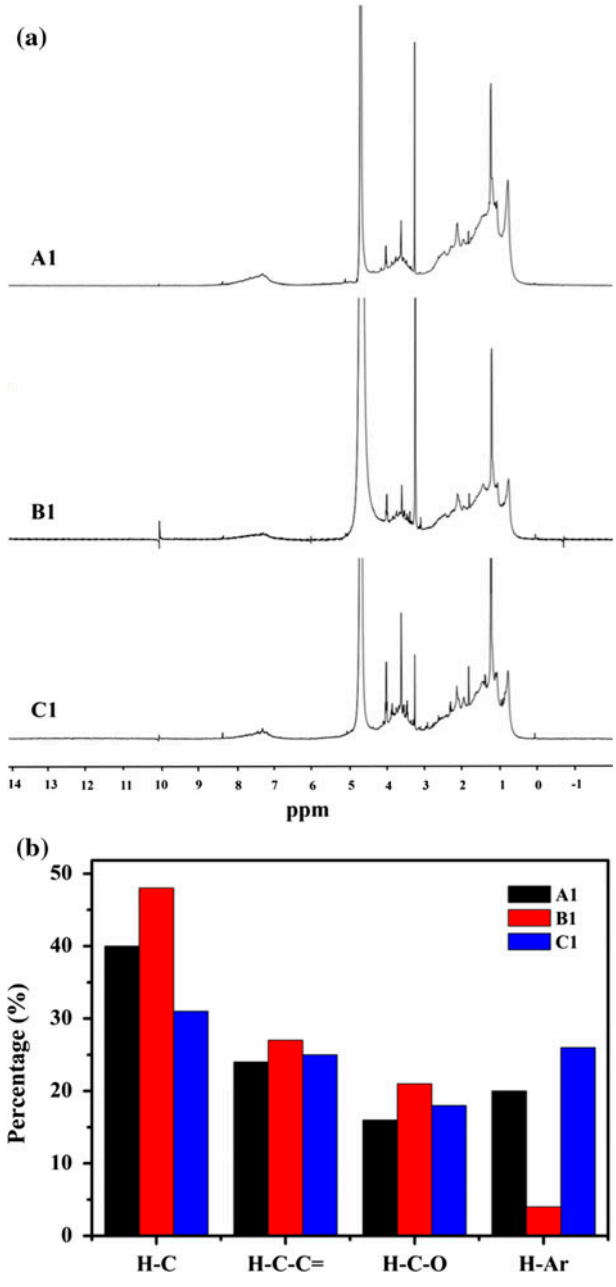

Fig. 6. (a) ^{1}H NMR spectra of CDOM in the extracted samples of *A*1, *B*1, and *C*1. The peak at 4.7 ppm indicates the water signal and (b) relative abundance of each type of protons, estimated as the partial integrals of the spectra reported in Fig. 6(a).

[19,20]. Previous studies demonstrated the presence of similar structures (aliphatic carbons singly bonded to one oxygen) in the water-soluble organic carbon (WSOC) isolated from atmospheric aerosols collected in a rural local near Averiro, Portugal [59] and in the organic fraction of aerosols collected during the wet season at Rondônia, Brazil [60].

Finally, the integration for the region of δ_H = 6.5–8.5 ppm demonstrated that samples *A*1 and *C*1 contained much higher aromatic substances (20 and 26%, respectively) than the sample *B*1 (4%), which were also supported by their corresponding $SUVA_{280}$ values. Particularly, it was roughly estimated that the content of the aromatic protons in this study were higher than other researchers found through the $SUVA_{280}$ values [5,19,20]. Furthermore, the distinct signals at δ_H = 7.2–7.3 and 7.6–7.8 ppm implied that the presence of aromatic rings contained both electron donor (e.g. phenolic groups) and electron acceptor (e.g. carbonyl and carboxyl) substituent [19].

4. Conclusions

This study presented a preliminary evaluation of the concentrations, compositions, and sources of CDOM collected from a typical residential area in Beijing, capital of China, using DOC, UV–visible spectroscopy, EEM fluorescence spectroscopy and ^{1}H NMR spectroscopy. (1) The CDOM in the stormwater runoff samples collected from three events possessed higher molecular weight, and the average molecular weight of CDOM followed the order of event *C* > event *B* > event *A*. (2) The higher $SUVA_{280}$ values of event *C* suggested more aromatic substances in event *C* than event *A* and *B*. (3) The results of EEM fluorescence spectroscopy demonstrated that UV humic-like substances were the major fluorophores components in the CDOM of runoff samples. The tryptophan protein-like components were also found in event *C*, which further confirmed that much larger molecular weight CDOM existed in event *C*. The fluorescence indices, like FI, HIX, BIX, were calculated to explore the sources of CDOM, suggesting both allochthonous and autochthonous sources contributed to the local CDOM, and their chemical properties were influenced by both anthropogenic and biogenic factors. (4) The results of ^{1}H NMR revealed that the CDOM in stormwater runoff samples mainly consisted of aliphatic chains and aromatic components with carbonyl, carboxyl and hydroxyl groups, CH_3-terminal methyls and CH_2 in alkyl chains. Considering that DOM could interact with various contaminants and even influence their transport and bioavailability, increasing efforts will be devoted to exploring the interactions between CDOM and coexisting contaminants (heavy metals and another organic substances) in stormwater runoff. And further investigations should be conducted to study the influences of CDOM in stormwater runoff to aquatic system, to guarantee the sustainability of city ecosystems.

Acknowledgments

We thank the financial support from the Beijing Natural Science Foundation (No. 8152013), the Importation & Development of High-Caliber Talents Project of Beijing Municipal Institutions (CIT&CD201404076), National Natural Science Foundation of China (No. 51478026), 2011 Project for Cooperation & Innovation under the Jurisdiction of Beijing Municipality, Open Research Fund Program of Key Laboratory of Urban Stormwater System and Water Environment (Ministry of Education), and 2011 Project for Cooperation & Innovation under the Jurisdiction of Beijing Municipality.

References

[1] P.R. Salve, H. Lohkare, T. Gobre, G. Bodhe, R.J. Krupadam, D.S. Ramteke, S.R. Wate, Characterization of chromophoric dissolved organic matter (CDOM) in rainwater using fluorescence spectrophotometry, Bull. Environ. Contam. Toxicol. 88 (2012) 215–218.
[2] C. Miller, K.G. Gordon, R.J. Kieber, J.D. Willey, P.J. Seaton, Chemical characteristics of chromophoric dissolved organic matter in rainwater, Atmos. Environ. 43 (2009) 2497–2502.
[3] P.G. Coble, Marine optical biogeochemistry: The chemistry of ocean color, Chem. Rev. 107 (2007) 402–418.
[4] R.G. Zepp, W.M. Sheldon, M.A. Moran, Dissolved organic fluorophores in southeastern US coastal waters: Correction method for eliminating Rayleigh and Raman scattering peaks in excitation–emission matrices, Mar. Chem. 89 (2004) 15–36.
[5] R.J. Kieber, R.F. Whitehead, S.N. Reid, J.D. Willey, P.J. Seaton, Chromophoric dissolved organic matter (CDOM) in rainwater, Southeastern North Carolina, USA, J. Atmos. Chem. 54 (2006) 21–41.
[6] S. Decesari, M. Facchini, S. Fuzzi, G. McFiggans, H. Coe, K. Bower, The water-soluble organic component of size-segregated aerosol, cloud water and wet depositions from Jeju Island during ACE-Asia, Atmos. Environ. 39 (2005) 211–222.
[7] M.C. Facchini, S. Decesari, M. Mircea, S. Fuzzi, G. Loglio, Surface tension of atmospheric wet aerosol and cloud/fog droplets in relation to their organic carbon content and chemical composition, Atmos. Environ. 34 (2000) 4853–4857.
[8] G. Kiss, E. Tombácz, H.C. Hansson, Surface tension effects of humic-like substances in the aqueous extract of tropospheric fine aerosol, J. Atmos. Chem. 50 (2005) 279–294.
[9] S. Memon, M.C. Paule, S.J. Park, B.Y. Lee, S. Kang, R. Umer, C.H. Lee, Monitoring of land use change impact on stormwater runoff and pollutant loading estimation in Yongin watershed Korea, Desalin. Water Treat. 51 (2013) 4088–4096.
[10] A. Goonetilleke, E. Thomas, S. Ginn, D. Gilbert, Understanding the role of land use in urban stormwater quality management, J. Environ. Manage. 74 (2005) 31–42.
[11] P.S. Santos, E.B. Santos, A.C. Duarte, Dissolved organic and inorganic matter in bulk deposition of a coastal urban area: An integrated approach, J. Environ. Manage. 145 (2014) 71–78.
[12] J.H. Lee, K.W. Bang, Characterization of urban stormwater runoff, Water Res. 34 (2000) 1773–1780.
[13] J.C. Jeon, K.H. Kwon, Y.J. Jung, M.J. Kang, K.S. Min, Characteristics of stormwater runoff from junkyard, Desalin. Water Treat. 53 (2015) 3039–3047.
[14] J.C. Han, X.L. Gao, Y. Liu, H.W. Wang, Y. Chen, Distributions and transport of typical contaminants in different urban stormwater runoff under the effect of drainage systems, Desalin. Water Treat. 52 (2014) 1455–1461.
[15] R. Kieber, S. Skrabal, B. Smith, J. Willey, Organic complexation of Fe(II) and its impact on the redox cycling of iron in rain, Environ. Sci. Technol. 39 (2005) 1576–1583.
[16] R.J. Kieber, S.A. Skrabal, C. Smith, J.D. Willey, Redox speciation of copper in rainwater: Temporal variability and atmospheric deposition, Environ. Sci. Technol. 38 (2004) 3587–3594.
[17] S.P. McElmurry, D.T. Long, T.C. Voice, Stormwater dissolved organic matter: Influence of land cover and environmental factors, Environ. Sci. Technol. 48 (2013) 45–53.
[18] C. Zhao, C.C. Wang, J.Q. Li, C.Y. Wang, P. Wang, Z.J. Pei, Dissolved organic matter in urban stormwater runoff at three typical regions in Beijing: Chemical composition, structural characterization and source identification, RSC Adv. 5 (2015) 73490–73500.
[19] P.S. Santos, M. Otero, R.M. Duarte, A.C. Duarte, Spectroscopic characterization of dissolved organic matter isolated from rainwater, Chemosphere 74 (2009) 1053–1061.
[20] P.S. Santos, E.B. Santos, A.C. Duarte, First spectroscopic study on the structural features of dissolved organic matter isolated from rainwater in different seasons, Sci. Total Environ. 426 (2012) 172–179.
[21] L. Yang, J. Hur, Critical evaluation of spectroscopic indices for organic matter source tracing via end member mixing analysis based on two contrasting sources, Water Res. 59 (2014) 80–89.
[22] J.T. Matos, S.M. Freire, R.M. Duarte, A.C. Duarte, Natural organic matter in urban aerosols: Comparison between water and alkaline soluble components using excitation-emission matrix fluorescence spectroscopy and multiway data analysis, Atmos. Environ. 102 (2015) 1–10.
[23] P.J. Seaton, R.J. Kieber, J.D. Willey, G.B. Avery, J.L. Dixon, Seasonal and temporal characterization of dissolved organic matter in rainwater by proton nuclear magnetic resonance spectroscopy, Atmos. Environ. 65 (2013) 52–60.
[24] X. Hao, A megacity held hostage: Beijing's conflict between water and economy, Water21 6 (2012) 39–42.
[25] C.L. Muller, A. Baker, R. Hutchinson, I.J. Fairchild, C. Kidd, Analysis of rainwater dissolved organic carbon compounds using fluorescence spectrophotometry, Atmos. Environ. 42 (2008) 8036–8045.
[26] J. Para, P.G. Coble, B. Charrière, M. Tedetti, C. Fontana, R. Sempéré, Fluorescence and absorption properties of chromophoric dissolved organic matter (CDOM) in coastal surface waters of the Northwestern

Mediterranean Sea (Bay of Marseilles, France), Biogeosci. Discuss. 7 (2010) 5675–5718.
[27] C.A. Stedmon, R. Bro, Characterizing dissolved organic matter fluorescence with parallel factor analysis: A tutorial, Limnol. Oceanogr. Methods 6 (2008) 572–579.
[28] D.M. McKnight, E.W. Boyer, P.K. Westerhoff, P.T. Doran, T. Kulbe, D.T. Andersen, Spectrofluorometric characterization of dissolved organic matter for indication of precursor organic material and aromaticity, Limnol. Oceanogr. 46 (2001) 38–48.
[29] R. Jaffé, J. Boyer, X. Lu, N. Maie, C. Yang, N. Scully, S. Mock, Source characterization of dissolved organic matter in a subtropical mangrove-dominated estuary by fluorescence analysis, Mar. Chem. 84 (2004) 195–210.
[30] A. Huguet, L. Vacher, S. Saubusse, H. Etcheber, G. Abril, S. Relexans, F. Ibalot, E. Parlanti, New insights into the size distribution of fluorescent dissolved organic matter in estuarine waters, Org. Geochem. 41 (2010) 595–610.
[31] A. Zsolnay, E. Baigar, M. Jimenez, B. Steinweg, F. Saccomandi, Differentiating with fluorescence spectroscopy the sources of dissolved organic matter in soils subjected to drying, Chemosphere 38 (1999) 45–50.
[32] A. Huguet, L. Vacher, S. Relexans, S. Saubusse, J.M. Froidefond, E. Parlanti, Properties of fluorescent dissolved organic matter in the Gironde Estuary, Org. Geochem. 40 (2009) 706–719.
[33] J. Amador, P.J. Milne, C.A. Moore, R.G. Zika, Extraction of chromophoric humic substances from seawater, Mar. Chem. 29 (1990) 1–17.
[34] P.S.M. Santos, R.M.B.O. Duarte, A.C. Duarte, Absorption and fluorescence properties of rainwater during the cold season at a town in Western Portugal, J. Atmos. Chem. 62 (2009) 45–57.
[35] R.M.B.O. Duarte, A.C. Duarte, Application of non-ionic solid sorbents (XAD Resins) for the isolation and fractionation of water-soluble organic compounds from atmospheric aerosols, J. Atmos. Chem. 51 (2005) 79–93.
[36] N. Senesi, T. Miano, M. Provenzano, G. Brunetti, Spectroscopic and compositional comparative characterization of I.H.S.S. reference and standard fulvic and humic acids of various origin, Sci. Total Environ. 81–82 (1989) 143–156.
[37] J. Peuravuori, K. Pihlaja, Molecular size distribution and spectroscopic properties of aquatic humic substances, Anal. Chim. Acta 337 (1997) 133–149.
[38] X.S. He, B.D. Xi, Y.H. Jiang, L.S. He, D. Li, H.W. Pan, S.G. Bai, Structural transformation study of water-extractable organic matter during the industrial composting of cattle manure, Microchem. J. 106 (2013) 160–166.
[39] J.N. Brown, B.M. Peake, Sources of heavy metals and polycyclic aromatic hydrocarbons in urban stormwater runoff, Sci. Total Environ. 359 (2006) 145–155.
[40] M.E. Tuccillo, Size fractionation of metals in runoff from residential and highway storm sewers, Sci. Total Environ. 355 (2006) 288–300.
[41] T. Jamieson, E. Sager, C. Guéguen, Characterization of biochar-derived dissolved organic matter using UV-visible absorption and excitation-emission fluorescence spectroscopies, Chemosphere 103 (2014) 197–204.
[42] C.A. Stedmon, S. Markager, H. Kaas, Optical properties and signatures of chromophoric dissolved organic matter (CDOM) in Danish coastal waters, Estuarine, Coastal Shelf Sci. 51 (2000) 267–278.
[43] J.R. Helms, A. Stubbins, J.D. Ritchie, E.C. Minor, D.J. Kieber, K. Mopper, Absorption spectral slopes and slope ratios as indicators of molecular weight, source, and photobleaching of chromophoric dissolved organic matter, Limnol. Oceanogr. 53 (2008) 955.
[44] J.L. Weishaar, G.R. Aiken, B.A. Bergamaschi, M.S. Fram, R. Fujii, K. Mopper, Evaluation of specific ultraviolet absorbance as an indicator of the chemical composition and reactivity of dissolved organic carbon, Environ. Sci. Technol. 37 (2003) 4702–4708.
[45] T. Klotzbücher, K. Kaiser, T.R. Filley, K. Kalbitz, Processes controlling the production of aromatic water-soluble organic matter during litter decomposition, Soil Biol. Biochem. 67 (2013) 133–139.
[46] T. Mattsson, P. Kortelainen, A. Räike, Export of DOM from boreal catchments: Impacts of land use cover and climate, Biogeochemistry 76 (2005) 373–394.
[47] J.D. Hosen, O.T. McDonough, C.M. Febria, M.A. Palmer, Dissolved organic matter quality and bioavailability changes across an urbanization gradient in headwater streams, Environ. Sci. Technol. 48 (2014) 7817–7824.
[48] A.H. Miguel, T.W. Kirchstetter, R.A. Harley, S.V. Hering, On-road emissions of particulate polycyclic aromatic hydrocarbons and black carbon from gasoline and diesel vehicles, Environ. Sci. Technol. 32 (1998) 450–455.
[49] P. Kjeldsen, M.A. Barlaz, A.P. Rooker, A. Baun, A. Ledin, T.H. Christensen, Present and long-term composition of MSW landfill Leachate: A review, Crit. Rev. Environ. Sci. Technol. 32 (2002) 297–336.
[50] C.L. Gigliotti, P.A. Brunciak, J. Dachs, T.R. Glenn, E.D. Nelson, L.A. Totten, S.J. Eisenreich, Air-water exchange of polycyclic aromatic hydrocarbons in the New York-New Jersey, USA, Harbor Estuary, Environ. Toxicol. Chem. 21 (2002) 235–244.
[51] C.L. Gigliotti, J. Dachs, E.D. Nelson, P.A. Brunciak, S.J. Eisenreich, Polycyclic aromatic hydrocarbons in the New Jersey coastal atmosphere, Environ. Sci. Technol. 34 (2000) 3547–3554.
[52] C.L. Gigliotti, L.A. Totten, J.H. Offenberg, J. Dachs, J.R. Reinfelder, E.D. Nelson, T.R. Glenn IV, S.J. Eisenreich, Atmospheric concentrations and deposition of polycyclic aromatic hydrocarbons to the mid-Atlantic East coast region, Environ. Sci. Technol. 39 (2005) 5550–5559.
[53] N. Hudson, A. Baker, D. Reynolds, Fluorescence analysis of dissolved organic matter in natural, waste and polluted waters—A review, River Res. Appl. 23 (2007) 631–649.
[54] K. Kaiser, R. Benner, Biochemical composition and size distribution of organic matter at the Pacific and Atlantic time-series stations, Mar. Chem. 113 (2009) 63–77.
[55] A. Nebbioso, A. Piccolo, Molecular characterization of dissolved organic matter (DOM): A critical review, Anal. Bioanal. Chem. 405 (2013) 109–124.
[56] S. Decesari, M.C. Facchini, S. Fuzzi, E. Tagliavini, Characterization of water-soluble organic compounds in atmospheric aerosol: A new approach, J. Geophys. Res. 105 (2000) 1481.

[57] S. Decesari, M. Facchini, E. Matta, F. Lettini, M. Mircea, S. Fuzzi, E. Tagliavini, J.P. Putaud, Chemical features and seasonal variation of fine aerosol water-soluble organic compounds in the Po Valley, Italy, Atmos. Environ. 35 (2001) 3691–3699.

[58] P. Schmitt-Kopplin, A. Gelencsér, E. Dabek-Zlotorzynska, G. Kiss, N. Hertkorn, M. Harir, Y. Hong, I. Gebefügi, Analysis of the unresolved organic fraction in atmospheric aerosols with ultrahigh-resolution mass spectrometry and nuclear magnetic resonance spectroscopy: Organosulfates as photochemical smog constituents†, Anal. Chem. 82 (2010) 8017–8026.

[59] R.M. Duarte, C.A. Pio, A.C. Duarte, Spectroscopic study of the water-soluble organic matter isolated from atmospheric aerosols collected under different atmospheric conditions, Anal. Chim. Acta 530 (2005) 7–14.

[60] S. Decesari, S. Fuzzi, M. Facchini, M. Mircea, L. Emblico, F. Cavalli, W. Maenhaut, X. Chi, G. Schkolnik, A. Falkovich, Characterization of the organic composition of aerosols from Rondônia, Brazil, during the LBA-SMOCC experiment and its representation through model compounds, Atmos. Chem. Phys. 6 (2006) 375–402.